

## Riemann $\zeta$ function from wave-packet dynamics

R. Mack,<sup>1</sup> J. P. Dahl,<sup>1,2</sup> H. Moya-Cessa,<sup>1,3</sup> W. T. Strunz,<sup>4</sup> R. Walser,<sup>1,5</sup> and W. P. Schleich<sup>1</sup>

<sup>1</sup>*Institut für Quantenphysik, Albert-Einstein-Allee 11, Universität Ulm, D-89069 Ulm, Germany*

<sup>2</sup>*Chemical Physics, Department of Chemistry, Technical University of Denmark, DTU 207, DK-2800 Kgs. Lyngby, Denmark*

<sup>3</sup>*Instituto Nacional de Astrofísica, Óptica y Electrónica, Apartado Postal 51 Y 216, 72000 Puebla, Mexico*

<sup>4</sup>*Institut für Theoretische Physik, Technische Universität Dresden, D-01062 Dresden, Germany*

<sup>5</sup>*Institut für Angewandte Physik, Technische Universität Darmstadt, D-64289 Darmstadt, Germany*

(Received 12 March 2010; published 29 September 2010)

We show that the time evolution of a thermal phase state of an anharmonic oscillator with logarithmic energy spectrum is intimately connected to the generalized Riemann  $\zeta$  function  $\zeta(s, a)$ . Indeed, the autocorrelation function at a time  $t$  is determined by  $\zeta(\sigma + i\tau, a)$ , where  $\sigma$  is governed by the temperature of the thermal phase state and  $\tau$  is proportional to  $t$ . We use the JWKB method to solve the inverse spectral problem for a general logarithmic energy spectrum; that is, we determine a family of potentials giving rise to such a spectrum. For large distances, all potentials display a universal behavior; they take the shape of a logarithm. However, their form close to the origin depends on the value of the Hurwitz parameter  $a$  in  $\zeta(s, a)$ . In particular, we establish a connection between the value of the potential energy at its minimum, the Hurwitz parameter and the Maslov index of JWKB. We compare and contrast exact and approximate eigenvalues of purely logarithmic potentials. Moreover, we use a numerical method to find a potential which leads to exact logarithmic eigenvalues. We discuss possible realizations of Riemann  $\zeta$  wave-packet dynamics using cold atoms in appropriately tailored light fields.

DOI: [10.1103/PhysRevA.82.032119](https://doi.org/10.1103/PhysRevA.82.032119)

PACS number(s): 03.65.Db, 42.50.-p

### I. INTRODUCTION

Factorization of numbers using a quantum computer [1], security of codes due to the use of single photons [2], and the similarity [3] of the statistics of the energy levels of a billiard and the zeros of the Riemann  $\zeta$  function point to an intimate connection between quantum mechanics [4] and number theory [5]. In the present article we connect two central ingredients of both theories: (i) The autocorrelation function [6], which describes the time evolution of a wave packet in quantum theory, and (ii) the Riemann  $\zeta$  function [7], which plays a crucial role in number theory due to the connection [5] between its nontrivial zeros and the distribution of the primes. We show that the autocorrelation function describing the time evolution of a thermal phase state [8] of an anharmonic oscillator with a logarithmic energy spectrum is determined by the generalized Riemann  $\zeta$  function [9] introduced by Adolf Hurwitz. In particular, we derive the form of the potential within the semiclassical (JWKB) approximation [10] and a numerical exact method and discuss possible realizations using cold atoms and light forces [11].

#### A. Inverse spectral problem

The development of ultrashort laser pulses [12] together with the progress in ion trap technology [13] and cavity quantum electrodynamics [14] has opened a new avenue in the observation of the time evolution of wave packets. Indeed, the motion of a Rydberg electron [15], the center-of-mass motion of an ion stored in a Paul trap [16] or an atom in a standing wave [17] together with the periodic exchange of excitation between an atom and the photon field in a high- $Q$  cavity [18] represent only a few examples of wave packets which are now almost routinely realized experimentally in many laboratories around the world. Central to these observations is the autocorrelation function representing the time-dependent overlap between the time-evolved state and the initial state of the quantum system

of interest. All experiments aforementioned have relied on the measurement of the autocorrelation function. Therefore, it is safe to say that this quantity is readily available.

In quantum mechanics the potential determines uniquely the energy spectrum. How can we determine the potential which generates a predetermined spectrum? This important question constitutes the so-called inverse problem [19] and has attracted much attention throughout the history of quantum mechanics. Today it is often attacked by constructing the unknown potential energy function from an analytical function with several adjustable parameters. The parameters are then varied until a satisfactory agreement between experimental and calculated energy levels or scattering phase shifts has been attained. If, however, a semiclassical description is judged to be sufficiently accurate, then explicit analytical methods are available. They have their origin in molecular spectroscopy of diatomic molecules and have been refined over the years. The basic semiclassical approach for solving the inverse problem is the Rydberg-Klein-Rees (RKR) method [20–22].

In the present article we pursue both approaches: We first use the RKR technique to obtain a potential implied by our logarithmic energy spectrum. Since this potential is only approximate, we then follow the numerical approach and find the exact potential using an iterative scheme based on the Hellmann-Feynman theorem [23–25].

#### B. Outline

Our article is organized as follows. In Sec. II we show that the autocorrelation function of a thermal phase state evolving in an anharmonic oscillator potential with a logarithmic energy spectrum

$$E_n \equiv \hbar\omega \ln[\gamma(n + a)] = \hbar\omega \ln(n + a) + \hbar\omega \ln \gamma \quad (1)$$

is determined by the generalized Riemann  $\zeta$  function. Here the constant  $\omega$  has the units of a frequency, and the dimensionless

parameter  $\gamma$  plays the role of a constant offset of the energy. The quantity  $a$  will later be connected to the Maslov index [26] of JWKB.

We then turn to the inverse spectral problem and determine a potential which gives rise to such a spectrum. Here we pursue analytical as well as numerical methods. In particular, in Sec. III we obtain within the JWKB approximation in one space dimension a family of potentials giving rise to an energy spectrum of the form of Eq. (1). In the neighborhood of the origin the potential can be approximated by that of a harmonic oscillator, but for large distances it is characterized by a logarithmic behavior. The value  $V_0$  of the potential at the origin, scaled in units of  $\hbar\omega$ , is connected to the parameter  $\gamma$  and to the Maslov index.

In Sec. IV we focus on a purely logarithmic potential and compare and contrast the desired energy eigenvalues given by Eq. (1) with the approximate ones. We find the familiar excellent agreement for large quantum numbers, but significant deviations for small quantum numbers, as expected by the limitations of the semiclassical approximation. This feature is unfortunate for our goal of realizing the generalized Riemann  $\zeta$  function, since the probability amplitudes corresponding to a thermal phase state put more weight on the small quantum numbers. For this reason we construct in Sec. V a potential leading to logarithmic energy eigenvalues using numerical methods starting from the JWKB potential. In Sec. VI we give a brief discussion of possible experimental realizations of Riemann  $\zeta$  wave-packet dynamics.

We conclude in Sec. VII with a summary of our results and an outlook. Here we emphasize that our approach is based on the Dirichlet representation of the Riemann  $\zeta$  function, which is only valid for the domain of complex space to the right of the line  $\text{Re } s = 1$ . As a consequence, the realization of the Riemann  $\zeta$  function by wave-packet dynamics is limited to this region only. We briefly outline an approach [27] for extending our considerations into the critical strip where the nontrivial zeros of the Riemann  $\zeta$  function are located. Here the entanglement of two quantum systems will play a crucial role.

In order to keep the article self-contained, we have introduced several appendixes which summarize concepts most relevant to the topic of our article. Although we focus on the quantum system of a nonrelativistic particle moving in a one-dimensional potential, we emphasize in Appendix A that our considerations are more general and can be applied to many different physical systems. For example, the atomic dynamics in the Jaynes-Cummings model [10] leads to expressions which under appropriate conditions [27] can be cast into the Riemann  $\zeta$  function. In Appendix B we briefly address the mathematical question of the uniqueness of the solution of the inverse spectral problem. Here we rely mainly on Ref. [28]. Moreover, Appendix C represents a brief summary of the RKR method. We rederive a closed-form expression for the excursion of the particle in terms of the spectral density. A crucial ingredient of the RKR method is the solution of the Abel integral equation. For the sake of completeness, we review in Appendix D its derivation and present two alternative but completely equivalent formulations. They provide us with a compact expression for the excursion in complete agreement with the results of Appendix C. In Appendix E we highlight important features of the purely logarithmic potential.

Moreover, we use Appendix F to review the Hellmann-Feynman theorem [23–25], which is at the very heart of the numerical work of Sec. V.

## II. RIEMANN STATE

In the present section we connect the concept of the autocorrelation function with the Riemann  $\zeta$  function. In particular, we show that for a quantum system with a logarithmic energy spectrum and an initial thermal phase state the autocorrelation function  $\mathcal{C}$  is given by the generalized [9] Riemann  $\zeta$  function.

### A. An intriguing connection

Throughout this article we consider the model system of a nonrelativistic particle of mass  $\mu$  moving in a potential  $V = V(x)$  of one space coordinate  $x$ . The energy eigenstates  $|n\rangle$  with energies  $E_n$  are assumed to form a discrete set numbered by  $n = 0, 1, 2, \dots$

The time evolution of a superposition

$$|\psi(0)\rangle = \sum_{n=0}^{\infty} \psi_n |n\rangle \quad (2)$$

of such energy eigenstates with probability amplitudes  $\psi_n$  reads

$$|\psi(t)\rangle = \sum_{n=0}^{\infty} \psi_n e^{-iE_n t/\hbar} |n\rangle. \quad (3)$$

As a consequence, the autocorrelation function

$$\mathcal{C}(t) \equiv \langle \psi(0) | \psi(t) \rangle \quad (4)$$

takes the form

$$\mathcal{C}(t) = \sum_{n=0}^{\infty} |\psi_n|^2 e^{-iE_n t/\hbar}, \quad (5)$$

where  $W_n \equiv |\psi_n|^2$  denotes the occupation probability of the  $n$ th energy level of the quantum system.

For the special example of the logarithmic energy spectrum [Eq. (1)], the autocorrelation function  $\mathcal{C}$  given by Eq. (5) takes the form

$$\mathcal{C}(t) = \sum_{n=0}^{\infty} |\psi_n|^2 e^{-i\omega t \ln[\gamma(n+a)]} \quad (6)$$

or

$$\mathcal{C}(t) = e^{-i\varphi(t)} \sum_{n=0}^{\infty} |\psi_n|^2 \frac{1}{(n+a)^{i\omega t}}, \quad (7)$$

with

$$\varphi(t) \equiv \omega t \ln \gamma. \quad (8)$$

It is interesting to compare this expression to the Dirichlet representation [9],

$$\zeta(s, a) \equiv \sum_{n=0}^{\infty} \frac{1}{(n+a)^s}, \quad (9)$$

of the generalized Riemann  $\zeta$  function of complex-valued argument  $s$  and the Hurwitz parameter  $a$  with  $0 < a \leq 1$ . This sum is convergent [9] for  $1 < \sigma \equiv \text{Re } s$ .

For the special choice

$$\psi_n \equiv \mathcal{N}_R (n+a)^{-\sigma/2} \quad (10)$$

of the probability amplitudes giving rise to the quantum state

$$|\psi_R\rangle \equiv \mathcal{N}_R \sum_{n=0}^{\infty} \frac{1}{(n+a)^{\sigma/2}} |n\rangle, \quad (11)$$

we find the autocorrelation function

$$\mathcal{C}(t) = |\mathcal{N}_R|^2 e^{-i\varphi(t)} \sum_{n=0}^{\infty} \frac{1}{(n+a)^{\sigma+i\omega t}}; \quad (12)$$

that is,

$$\mathcal{C}(t) = |\mathcal{N}_R|^2 e^{-i\varphi(t)} \zeta(\sigma + i\omega t, a). \quad (13)$$

Hence, the time evolution of  $|\psi_R\rangle$  expressed by the autocorrelation function  $\mathcal{C}(t)$  and given by Eq. (13) reads out the generalized Riemann  $\zeta$  function along a line  $\text{Re } s = \sigma$  in complex space which is parallel to the imaginary axis. For this reason we have included a subscript R on the state  $|\psi_R\rangle$  and refer to it as *Riemann state*.

The normalization constant  $\mathcal{N}_R$  follows from the relation

$$\langle \psi_R | \psi_R \rangle = |\mathcal{N}_R|^2 \sum_{n=0}^{\infty} \frac{1}{(n+a)^\sigma} = |\mathcal{N}_R|^2 \zeta(\sigma, a) = 1 \quad (14)$$

and is determined by the real part  $\sigma$  of the argument  $s$  of  $\zeta$ .

When we substitute  $|\mathcal{N}_R|^2$  from Eq. (14) into Eq. (13), we find the compact expression

$$\mathcal{C}(t) = e^{-i\omega t \ln \gamma} \frac{\zeta(\sigma + i\omega t, a)}{\zeta(\sigma, a)} \quad (15)$$

for the autocorrelation function of the Riemann state.

### B. Thermal phase states

In order to gain more insight into the Riemann state  $|\psi_R\rangle$ , we express the probability amplitudes  $\psi_n$  given by Eq. (10) in terms of the logarithmic energy spectrum  $E_n$  determined by Eq. (1). For this purpose we note the identity

$$\psi_R = \mathcal{N}_R e^{\frac{\sigma}{2} \ln \gamma} e^{-\frac{\sigma}{2} \ln[\gamma(n+a)]} \quad (16)$$

and the Riemann state [Eq. (11)] takes the form

$$|\psi_R\rangle = \mathcal{N} \sum_{n=0}^{\infty} \exp\left(-\frac{1}{2} \frac{\sigma}{\hbar\omega} E_n\right) |n\rangle, \quad (17)$$

where  $\mathcal{N} \equiv \mathcal{N}_R \exp(\frac{\sigma}{2} \ln \gamma)$ .

We note that this state has been extensively discussed [8,29] in the context of a harmonic oscillator. Indeed, the thermal phase state

$$|\psi_{\text{ph}}\rangle_{\text{os}} \equiv \mathcal{N}_{\text{ph}} \sum_{n=0}^{\infty} \exp\left(-\frac{1}{2} \frac{\hbar\omega}{k_B T} n\right) |n\rangle_{\text{os}} \quad (18)$$

of temperature  $T$  which is a superposition of energy eigenstates  $|n\rangle_{\text{os}}$  of the harmonic oscillator can be cast in the form

$$|\psi_{\text{ph}}\rangle_{\text{os}} \equiv \mathcal{N}^{(\text{os})} \sum_{n=0}^{\infty} \exp\left(-\frac{1}{2} \frac{1}{k_B T} E_n^{(\text{os})}\right) |n\rangle_{\text{os}}, \quad (19)$$

with the energies

$$E_n^{(\text{os})} = \hbar\omega(n + \frac{1}{2}). \quad (20)$$

Here  $\mathcal{N}^{(\text{os})} \equiv \mathcal{N}_{\text{ph}} \exp(\frac{\hbar\omega}{4k_B T})$  and  $k_B$  denotes the Boltzmann constant.

Obviously, the Riemann state [Eq. (17)] is a thermal phase state in the anharmonic oscillator with the logarithmic energy spectrum [Eq. (1)]. This analysis even allows us to attribute a physical meaning to the real part  $\sigma$  of the argument  $s$  of the Riemann  $\zeta$  function. Indeed, a comparison between Eqs. (17) and (19) provides us with the identification

$$\sigma \equiv \frac{\hbar\omega}{k_B T}. \quad (21)$$

Hence,  $\sigma$  is the ratio of the energy unit  $\hbar\omega$  of the anharmonic oscillator to the thermal energy  $k_B T$ .

It is important to distinguish the pure Riemann state  $|\psi_R\rangle$  defined by Eq. (17) and giving rise to the density operator

$$\hat{\rho}_R = |\mathcal{N}|^2 \sum_{m,n=0}^{\infty} \exp\left[-\frac{E_m + E_n}{2k_B T}\right] |m\rangle\langle n| \quad (22)$$

from the mixed thermal state

$$\hat{\rho}_{\text{th}} \equiv |\mathcal{N}|^2 \sum_{n=0}^{\infty} \exp\left(-\frac{E_n}{k_B T}\right) |n\rangle\langle n|. \quad (23)$$

Both density operators enjoy the same diagonal elements. However, the Riemann state is a coherent superposition and therefore  $\hat{\rho}_R$  also contains off-diagonal elements. They reflect a preferred direction in phase space. Indeed, the main positive contribution of the Wigner function is aligned along the  $x$  axis. In contrast, the thermal state [Eq. (23)] is an incoherent superposition and does not have a preferred direction in phase space. For this reason the thermal state does not undergo any time evolution in the anharmonic oscillator, whereas the Riemann state does.

We conclude by noting that apart from their different eigenstates,  $|n\rangle_{\text{os}}$  versus  $|n\rangle$ , and their different normalization constants,  $\mathcal{N}_R$  versus  $\mathcal{N}_{\text{ph}}$ , the thermal phase states

$$|\psi_R\rangle = \mathcal{N}_R \sum_{n=0}^{\infty} \exp\left[-\frac{\sigma}{2} \ln(n+a)\right] |n\rangle \quad (24)$$

and

$$|\psi_{\text{ph}}\rangle_{\text{os}} = \mathcal{N}_{\text{ph}} \sum_{n=0}^{\infty} \exp\left[-\frac{\sigma}{2} n\right] |n\rangle_{\text{os}} \quad (25)$$

of the anharmonic and the harmonic oscillator following from Eqs. (11) and (18) transform into each other when we make the substitution  $n \rightarrow \ln(n+a)$ .

### III. CONSTRUCTION OF POTENTIAL: SEMICLASSICAL APPROACH

Next we address the question of how to find a quantum system which displays the logarithmic energy spectrum [Eq. (1)]. For this purpose we consider the quantum motion of a particle of mass  $\mu$  in a one-dimensional potential  $V = V(x)$  and determine  $V$  such that a logarithmic energy spectrum

emerges. Our main tool is the RKR method [20] of JWKB as summarized in Ref. [21] and Appendix C.

### A. Implicit expression for potential

We start by recalling from Appendix C the relation

$$X(E) = \sqrt{\frac{2\hbar^2}{\mu}} \int_{V_0}^E dE' \frac{1}{\sqrt{E-E'}} \frac{dn(E')}{dE'} \quad (26)$$

connecting the excursion

$$X(E) \equiv x_2(E) - x_1(E) \quad (27)$$

of the motion between the two turning points  $x_1(E) < x_2(E)$  of the particle of energy  $E$  with the inverse spectrum  $n = n(E)$ . Here  $V_0$  is the value of  $V(x)$  at the bottom of the potential well. Moreover, we assume that  $V$  has a single minimum and grows monotonically on each side.

When we substitute the inverse spectrum

$$n(E) = \frac{1}{\gamma} e^{E/\hbar\omega} - a, \quad (28)$$

following from Eq. (1), into Eq. (26) and perform the differentiation, we find

$$X(E) = \frac{1}{\gamma} \sqrt{\frac{2\hbar^2}{\mu}} \int_{V_0}^E d \left( \frac{E'}{\hbar\omega} \right) \frac{e^{E'/(\hbar\omega)}}{\sqrt{E-E'}}, \quad (29)$$

which with the substitution

$$\theta^2 \equiv \frac{E-E'}{\hbar\omega} \quad (30)$$

leads us to

$$X(E) = \frac{1}{\gamma\kappa} e^{E/\hbar\omega} \operatorname{erf} \left( \sqrt{\frac{E-V_0}{\hbar\omega}} \right). \quad (31)$$

Here we have introduced the abbreviation

$$\kappa \equiv \sqrt{\frac{\mu\omega}{2\pi\hbar}} \quad (32)$$

and have recalled the error function

$$\operatorname{erf}(y) \equiv \frac{2}{\sqrt{\pi}} \int_0^y d\theta e^{-\theta^2}. \quad (33)$$

Equation (31) provides us with the excursion  $X$  for a given energy  $E$ . Since  $X$  is the separation of the two turning points, this dependence on  $E$  yields the potential  $V(x)$ .

It is important to note that the excursion does not determine the potential uniquely. We have still some degrees of freedom, which do not alter the semiclassical energy levels. Indeed, when we assume the potential to be symmetric around  $x = 0$ , the excursion is twice the coordinate  $x$  and the potential  $V$  follows from the implicit equation

$$2\gamma\kappa|x| = e^{V(x)/\hbar\omega} \operatorname{erf} \left( \sqrt{\frac{V(x)-V_0}{\hbar\omega}} \right). \quad (34)$$

In this relation the parameters  $\omega$  and  $\gamma$  of the logarithmic energy spectrum [Eq. (1)] reappear. Moreover, the constant  $\kappa$  containing the properties of the particle such as the mass  $\mu$  multiplies the coordinate  $x$ . It is interesting that the constant  $a$  of the spectrum is missing in Eq. (34) but the value  $V_0$  of the

potential at the origin is present. Since no condition restricts  $V_0$ , Eq. (34) defines a family of potentials  $V$  parameterized by  $V_0$ . In order to bring out this fact most clearly, we denote the potential as  $V(x; V_0)$ .

### B. Explicit approximate expressions for potential

Next we derive explicit but approximate expressions for the potential  $V$  defined so far only implicitly by Eq. (34). For this purpose we consider two limiting cases of  $V$ .

When  $V - V_0 \ll \hbar\omega$  we can approximate the exponential function in Eq. (34) as  $\exp[V_0/(\hbar\omega)]$  and the error function as  $\operatorname{erf}(y) \cong 2y/\sqrt{\pi}$ . As a result, Eq. (34) leads us to

$$V(x; V_0) \cong V_0 + \frac{1}{2}\mu\omega_{\text{eff}}^2 x^2. \quad (35)$$

Hence, the potential  $V$  close to the origin is that of a harmonic oscillator with the effective frequency

$$\omega_{\text{eff}}(V_0) \equiv \gamma e^{-V_0/\hbar\omega} \omega \quad (36)$$

determined by  $\gamma$  and the minimal energy  $V_0$ .

In the case of  $\hbar\omega \ll V - V_0$  we can approximate  $\operatorname{erf}(y) \approx 1$ , which yields

$$V(x) \cong \hbar\omega \ln(2\gamma\kappa|x|). \quad (37)$$

For large distances the potential behaves like a logarithm.

In the intermediate regime of  $x$  we need to solve the implicit equation [Eq. (34)] by numerical methods to arrive at the potential  $V(x; V_0)$  shown in Figs. 1 and 2.

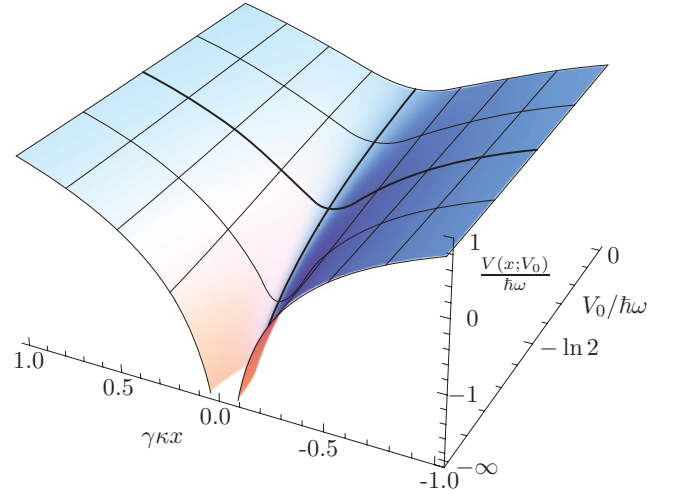


FIG. 1. (Color online) Potential  $V = V(x; V_0)$  for a nonrelativistic particle of mass  $\mu$  giving rise to a logarithmic energy spectrum  $E_n = \hbar\omega \ln[\gamma(n+a)]$  according to the RKR method. Here we display  $V$  in units of  $\hbar\omega$  in its dependence on the dimensionless position  $\gamma\kappa x$  and the value  $V_0/\hbar\omega$  of  $V$  at  $x = 0$ . The parameters  $\gamma$  and  $a$  of the spectrum determine via Eq. (40) the value  $V_0$ . At the origin the potential is approximately quadratic. For large values of  $\gamma\kappa|x|$  it increases logarithmically. In the limit of  $V_0 \rightarrow -\infty$  we obtain a purely logarithmic potential with a singularity at  $x = 0$ .

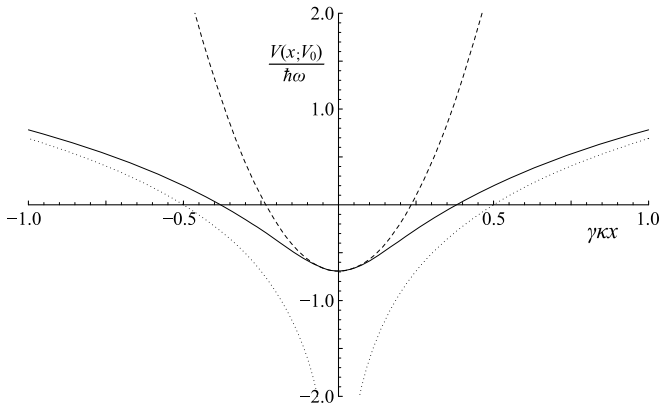


FIG. 2. Comparison between the RKR potential  $V(x; V_0)$  determined from Eq. (34) (depicted by the solid curve) and the approximations for small or large values of the dimensionless position  $\gamma\kappa x$  given by Eqs. (35) or (37) (represented by dashed or dotted lines, respectively). The potential is scaled in units of  $\hbar\omega$  and we have chosen a value of  $V_0 = -\hbar\omega \ln 2$ .

### C. Connection among $V_0$ , $a$ , and $\alpha$

In Appendix C we show that the minimal value  $V_0$  of  $V$  is connected to the Maslov index  $\alpha$  of the JWKB approximation by the relation

$$n(V_0) + \alpha = 0, \quad (38)$$

which for the logarithmic spectrum Eq. (1) with Eq. (28) takes the form

$$\frac{1}{\gamma} e^{V_0/\hbar\omega} - a + \alpha = 0. \quad (39)$$

Since the potential determined by Eq. (34) is symmetric, each turning point contributes to the Maslov index with  $1/4$  leading to  $\alpha = 1/2$ . As a consequence, we arrive at

$$\frac{V_0}{\hbar\omega} = \ln \left[ \gamma \left( a - \frac{1}{2} \right) \right], \quad (40)$$

which when substituted into the implicit expression Eq. (34) for the potential yields

$$2\gamma\kappa|x| = e^{V(x)/\hbar\omega} \operatorname{erf} \left( \sqrt{\frac{V(x)}{\hbar\omega} - \ln \left[ \gamma \left( a - \frac{1}{2} \right) \right]} \right). \quad (41)$$

Now all parameters of the energy spectrum [Eq. (1)] appear in this equation and the potential is uniquely determined.

We conclude by noting that, due to Eq. (40), the effective frequency  $\omega_{\text{eff}}$  [Eq. (36)] of the harmonic oscillator potential near  $x = 0$  takes the form

$$\omega_{\text{eff}} = \frac{\omega}{a - 1/2}. \quad (42)$$

For  $a \rightarrow 1/2$  this frequency approaches infinity.

### D. Tuning the Hurwitz parameter

So far we have considered the inverse spectral problem; that is, we have started from the logarithmic spectrum [Eq. (1)] and have obtained the potential  $V(x)$  by the implicit equation [Eq. (41)]. We came across this problem because of the connection [Eq. (15)] between the generalized Riemann

$\zeta$  function  $\zeta = \zeta(s, a)$  defined by Eq. (9) and the autocorrelation function [Eq. (4)] of an anharmonic oscillator with a logarithmic spectrum.

In  $\zeta(s, a)$  the Hurwitz parameter  $a$  makes its appearance. It is possible to use the constraint Eq. (40) to tune  $a$  by choosing the minimal value  $V_0$  of the potential; that is,

$$a = \frac{1}{2} + \frac{1}{\gamma} e^{V_0/\hbar\omega}. \quad (43)$$

Since the second term in this equation is always positive, we can cover the domain of  $1/2 \leq a$ . We find  $a = 1/2$  for  $V_0 = -\infty$ .

In order to also get access to the range  $0 < a < 1/2$ , we note [9] the relation

$$\zeta(s, a) = \frac{1}{a^s} + \zeta(s, a + 1), \quad (44)$$

which follows from the definition [Eq. (9)] of  $\zeta(s, a)$ .

We conclude by noting that Eq. (39) suggests another method of tuning  $a$ . This idea relies on constructing a quantum system in which the Maslov index  $\alpha$  can be “engineered,” that is, chosen at will. Indeed, we recall from Ref. [30] that in appropriate potentials the Maslov index can be different from the one predicted by the straightforward application of JWKB. However, the implementation of this approach to construct the appropriate potential which would achieve the generalized Riemann  $\zeta$  function goes beyond the scope of the present article.

## IV. PURELY LOGARITHMIC POTENTIAL

We now consider the time-independent Schrödinger equation for the potential which emerges from the implicit definition [Eq. (34)] of  $V(x; V_0)$  for  $V_0 \rightarrow -\infty$ . In this limit the argument of the error function becomes infinite and the error function takes on the value of unity. As a result we can now solve Eq. (34) for  $V$ , which takes the form

$$V(x; -\infty) \equiv U(x) = \hbar\omega \ln(2\gamma\kappa|x|). \quad (45)$$

We note that  $U(x)$  is identical to  $V(x; V_0)$  for large values of  $x$ . However, in contrast to  $V(x; V_0)$  the potential  $U(x)$  is singular at the origin.

In this section we discuss the eigenvalue spectrum of the time-independent Schrödinger equation

$$\left[ \frac{\hbar^2}{2\mu} \frac{d^2}{dx^2} + E - \hbar\omega \ln(2\gamma\kappa|x|) \right] u(x) = 0 \quad (46)$$

corresponding to  $U$ . For this purpose we first solve Eq. (46) numerically and then compare the so-obtained eigenvalues with the ones obtained from a JWKB analysis. For a summary of some of the unusual properties of the solution of the Schrödinger equation [Eq. (46)] for this purely logarithmic potential, we refer to Appendix E.

### A. Numerically exact eigenvalues

Many numerical techniques for integrating a Schrödinger equation with a singular potential offer themselves. We employ the Störmer-Numerov method [31] to obtain the exact energy spectrum corresponding to  $U$ .

TABLE I. Comparison between the energy eigenvalues of the purely logarithmic potential [Eq. (45)], obtained by different methods and in two distinct spatial domains accessible to the particle. Starting from the left, the second and third columns correspond to a particle experiencing the complete position axis. The fourth and fifth columns correspond to a particle being restricted to the positive axis only. The second column summarizes exact eigenvalues  $\tilde{E}_n^{(\text{ex})}$  obtained by numerically integrating Eq. (48). The third column represents the JWKB approximation  $\tilde{E}_n^{(-+)}$  of these energies given by Eq. (51). For the confined particle, only the odd eigenfunctions of the unrestricted particle survive. Here we summarize two calculations: In the fourth column we present the expression  $\tilde{E}_s^{(+)}$ , given by Eq. (53), and the fifth column shows the energies  $\tilde{E}_s^{(\text{L})}$  resulting from a numerical calculation in JWKB approximation after the addition of a repulsive centrifugal potential, as suggested by a Langer correction [Eq. (54)].

$n$	$\tilde{E}_n^{(\text{ex})}$	$\tilde{E}_n^{(-+)}$	$\tilde{E}_s^{(+)}$	$\tilde{E}_s^{(\text{L})}$	$s$
0	-1.795 524	-1.386 294			
1	-0.221 179	-0.287 682	-0.287 682	-0.212 045	0
2	0.192 559	0.223 144			
3	0.581 930	0.559 616	0.559 616	0.585 290	1
4	0.796 917	0.810 930			
5	1.024 103	1.011 600	1.011 600	1.025 946	2
6	1.169 875	1.178 655			
7	1.330 198	1.321 755	1.321 755	1.331 394	3
8	1.440 630	1.446 919			
9	1.564 416	1.558 144	1.558 144	1.565 276	4
21	2.377 198	2.374 905	2.374 905	2.377 464	10
41	3.033 586	3.032 546	3.032 546	3.033 689	20
61	3.426 543	3.425 889	3.425 889	3.426 602	30
81	3.707 925	3.707 455	3.707 455	3.707 964	40
101	3.927 275	3.926 911	3.926 911	3.927 304	50
201	4.612 807	4.612 642	4.612 642	4.612 818	100

For this purpose we first introduce the scaled energy  $\tilde{E} \equiv E/\hbar\omega$  and the dimensionless position

$$\xi \equiv \sqrt{\frac{\mu\omega}{\hbar}} x, \quad (47)$$

leading to the equation

$$\left[ \frac{1}{2} \frac{d^2}{d\xi^2} + \tilde{E} - \ln \left( \sqrt{\frac{2}{\pi}} \gamma |\xi| \right) \right] u(\xi) = 0. \quad (48)$$

In Table I we list the energy eigenvalues  $\tilde{E}_n^{(\text{ex})}$  obtained for  $\gamma = 1/2$  by numerically integrating Eq. (48).

### B. Approximate eigenvalues

Next we compare the numerically exact eigenvalues  $\tilde{E}_n^{(\text{ex})}$  with the ones predicted by JWKB. We start by recalling that Eq. (39) connects the parameter  $a$  of the desired energy spectrum [Eq. (1)] to the Maslov index  $\alpha$  and the potential energy  $V_0$  at the origin. For  $V_0 = -\infty$  Eq. (39) reduces to

$$a = \alpha, \quad (49)$$

and we obtain the expression

$$\tilde{E}_n = \ln[\gamma(n + \alpha)] \quad (50)$$

for the energy spectrum with  $n = 0, 1, 2, \dots$

### 1. Unrestricted motion

The Schrödinger equation [Eq. (48)] has a singularity at  $\xi = 0$ . When we allow the particle to cross this singularity, we have two turning points resulting in a Maslov index  $\alpha = 2 \times 1/4 = 1/2$ . In this case the energy spectrum for a particle probing the negative as well as the positive axis predicted by the JWKB expression [Eq. (50)] reads

$$\tilde{E}_n^{(-+)} = \ln \left[ \gamma \left( n + \frac{1}{2} \right) \right]. \quad (51)$$

In the third column of Table I we list the eigenvalues  $\tilde{E}_n^{(-+)}$  for  $\gamma = 1/2$ . We note that in general the agreement with the exact ones is rather poor.

### 2. Restricted motion

In the JWKB method it is dangerous [32] to ignore the singularity at  $\xi = 0$  and to extend  $\xi$  toward negative values. The variable  $\xi$  must be confined to the interval  $0 \leq \xi < \infty$ . The poor man's way to treat the singularity is to set up a hard wall. The intelligent way is to invoke the Langer correction [33]. We now discuss both cases.

*a. Hard wall.* The boundary condition  $u(\xi) = 0$  at  $\xi = 0$  selects from Eq. (50) only the odd values of  $n$ , that is,  $n = 2s + 1$ . As a result, the energy spectrum becomes

$$\tilde{E}_s^{(+)} = \ln \left[ 2\gamma \left( s + \frac{1}{2} + \frac{\alpha}{2} \right) \right], \quad (52)$$

with  $s = 0, 1, 2, \dots$

Since  $\alpha = 1/2$  we arrive at the energy spectrum

$$\tilde{E}_s^{(+)} = \ln \left[ 2\gamma \left( s + \frac{3}{4} \right) \right] \quad (53)$$

predicted by JWKB for the motion of a particle restricted to the positive  $\xi$  axis only. In the fourth column of Table I we list the dimensionless eigenvalues  $\tilde{E}_s^{(+)}$  for  $\gamma = 1/2$ .

*b. Langer correction.* We obtain a much better agreement when we include the Langer correction [33], which corresponds to adding the repulsive potential  $\hbar^2/(8\mu x^2)$  to the Schrödinger equation [Eq. (46)]. The corresponding Schrödinger equation in dimensionless units then reads

$$\left[ \frac{1}{2} \frac{d^2}{d\xi^2} + \tilde{E}^{(+)} - \frac{1}{8\xi^2} - \ln \left( \sqrt{\frac{2}{\pi}} \gamma |\xi| \right) \right] u(\xi) = 0. \quad (54)$$

In the fifth column of Table I we present the dimensionless eigenvalues  $\tilde{E}_s^{(\text{L})}$  obtained by the JWKB method including the Langer correction. Now we obtain a much better agreement with the exact values corresponding to the odd wave functions.

## V. CONSTRUCTION OF POTENTIAL: NUMERICAL APPROACH

In Sec. III we use the RKR method to determine the potential which leads to the logarithmic energy spectrum given by Eq. (1). Since this method is approximate, we use in the present section a perturbation theory based on the Hellmann-Feynman theorem to obtain numerically the exact potential which provides us with the desired logarithmic energy spectrum. For more details on this method, see Appendix F.

### A. Outline of the algorithm

Our starting point is the approximate potential  $V^{(j)}(x)$ . Here the superscript  $j$  denotes the  $j$ th iteration.

Next we solve the time-independent Schrödinger equation

$$\left\{ \frac{d^2}{dx^2} + \frac{2\mu}{\hbar^2} [E_m^{(j)} - V^{(j)}(x)] \right\} \varphi_m^{(j)}(x) = 0 \quad (55)$$

for the energy wave functions  $\varphi_m^{(j)}$  and the eigenvalues  $E_m^{(j)}$ .

In order to obtain the desired energy spectrum  $E_m^{(d)}$ , we add a correction potential  $\delta V(x; \boldsymbol{\beta}^{(j)})$  parameterized by the vector  $\boldsymbol{\beta}^{(j)}$  to  $V^{(j)}(x)$ . We determine the components  $\beta_n^{(j)}$  of  $\boldsymbol{\beta}^{(j)}$  from the linear system of equations

$$\sum_n M_{mn}^{(j)} \beta_n^{(j)} = E_m^{(d)} - E_m^{(j)} \quad (56)$$

with the matrix

$$M_{mn}^{(j)} \equiv \int dx |\varphi_m^{(j)}(x)|^2 \frac{\partial}{\partial \beta_n} \delta V(x; \boldsymbol{\beta}) \Big|_{\boldsymbol{\beta}=0}. \quad (57)$$

These parameters determine the new potential

$$V^{(j+1)}(x) = V^{(j)}(x) + \delta V(x; \boldsymbol{\beta}^{(j)}), \quad (58)$$

which serves as the input for the  $j + 1$  iteration.

We still have to determine an appropriate parametrization of the correction potential. For the present problem it is convenient to choose the form

$$\delta V(x; \boldsymbol{\beta}) = \sum_l \beta_l |\varphi_l^{(j)}(x)|^2, \quad (59)$$

which leads to the symmetric matrix

$$M_{mn}^{(j)} = \int dx |\varphi_m^{(j)}(x)|^2 |\varphi_n^{(j)}(x)|^2. \quad (60)$$

Indeed, it is useful to parametrize the potential  $\delta V$  in terms of the probability density  $|\varphi_l^{(j)}|^2$  rather than the probability amplitudes  $\varphi_l^{(j)}$ . In this case the matrix  $M_{mn}^{(j)}$  is symmetric.

### B. Application: Logarithmic spectrum

We illustrate the algorithm introduced in the preceding section to obtain the potential corresponding to the logarithmic energy spectrum [Eq. (1)] for the choice of the parameters  $a = \gamma = 1$ . In this case we have the eigenvalues

$$E_n = \hbar\omega \ln(n + 1), \quad (61)$$

with  $n = 0, 1, 2, \dots$ . Such a spectrum has also been investigated [34] on the basis of partial supersymmetries.

We start the iteration with the RKR potential  $V^{(0)}$  discussed in Sec. III. Our algorithm converges toward the potential shown in Fig. 3. We note a substantial deviation between the RKR potential and the numerically exact one, which, however, for larger values of  $x$  ceases to exist.

## VI. SCENARIOS FOR AN EXPERIMENTAL REALIZATION

We now briefly address the question of how to create a logarithmic potential in an experiment. Here the number  $D$  of dimensions the particle is allowed to experience will play

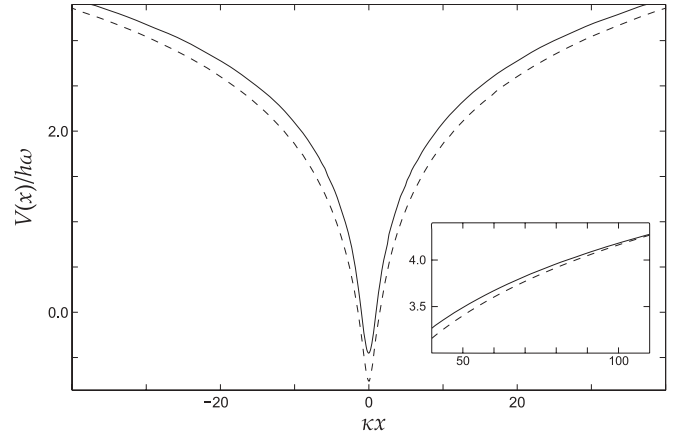


FIG. 3. Comparison between the numerically exact potential (solid line) leading to the energy spectrum  $E_n = \hbar\omega \ln(n + 1)$  and the RKR potential (dashed line). The two potentials are substantially different. However, for larger distances the deviation becomes less important, as shown by the inset. Here we have chosen the parameters  $V_0 = -\hbar\omega \ln 2$  and  $a = \gamma = 1$ . Moreover, we have expressed the potentials in units of  $\hbar\omega$ . The dimensionless position variable is given by  $\kappa x$ .

an important role, as discussed for the case of the purely logarithmic potential in Appendix E.

We start by recalling that light forces acting on cold atoms are a promising tool in realizing arbitrary prescribed potentials. Indeed, a laser field with an intensity profile of the form of the desired potential interacting nonresonantly with an atom enforces this very potential on its center-of-mass motion. Holographic optical beam shapers can create [35] a wide variety of mode functions for the laser field. This technique is now used routinely in laboratories.

Another possibility for creating a logarithmic potential is to take advantage of the Coulomb potential in  $D = 2$  dimensions. Here the solution of the Poisson equation is not a  $1/r$  potential but rather displays a logarithmic dependence on the radius. In the field of electron optics the electron biprism [36] relies on such a two-dimensional logarithmic potential.

Unfortunately, we have to include also a centrifugal potential with  $1/r^2$  dependence. Even for a vanishing angular momentum do we obtain a nonvanishing  $1/r^2$  potential which in this case is even attractive [37]. Thus, the case of  $D = 2$  automatically provides the logarithmic potential together with the hard wall at  $r = 0$  but also brings in an unwanted term which dominates the logarithmic behavior for short distances.

However, we recall that in  $D = 3$  the centrifugal potential vanishes for quantum states of zero angular momentum, that is, for  $s$  waves. The hard wall at  $r = 0$  is still present due to the spherical symmetry of the problem. However, we now need to create the three-dimensional logarithmic potential using an appropriate laser intensity distribution, as discussed before. This approach seems to be possible with current technology.

## VII. SUMMARY AND OUTLOOK

There exists extensive literature on the problem [38] of constructing a Hamiltonian whose eigenvalues are determined by the nontrivial zeros of the Riemann  $\zeta$  function. However,

these attempts to verify the Hilbert-Pólya conjecture [39] are fundamentally different from our approach to connect quantum mechanics and the Riemann  $\zeta$  function. Indeed, our goal was to construct an analog computer for the Riemann  $\zeta$  function. For this purpose, we have studied the autocorrelation function  $\mathcal{C}$  of a quantum state propagating in an anharmonic oscillator potential. The connection to the Riemann  $\zeta$  function is made through its Dirichlet representation. Indeed, a direct comparison between the expressions for  $\mathcal{C}$  and  $\zeta$  leads to the logarithmic energy spectrum of the oscillator, as well as the probability amplitudes of the evolving thermal phase state.

It is interesting to note that the thermal phase state has already once played an important role in quantum optics. In the context of the old question [40] of a Hermitian operator corresponding to the phase variable, thermal phase states have provided substantial insight into the variational problem of minimizing the phase uncertainty for a given number of photons [41]. Optimal phase states [42] arise in interferometric measurements at the quantum limit.

We have then devoted a substantial portion of our article to the problem of finding the oscillator potential with a logarithmic spectrum. In this sense our approach is reminiscent of the one of Hilbert and Pólya. We also have to solve an inverse spectral problem. Indeed, we search for a Hamiltonian whose eigenvalues depend logarithmically on the quantum number. Obviously, this spectrum is distinctly different from the sought-after Hilbert-Pólya one given by the nontrivial zeros of the Riemann  $\zeta$  function.

We emphasize that our ansatz of an analog computer for  $\zeta$  rests on the Dirichlet representation. However, this sum is only convergent for arguments  $s$  of  $\zeta$  with  $1 < \text{Re } s$ . In our language of evolving quantum states the requirement of convergence translates into the normalization condition of the state. In particular, the occupation probabilities of the individual energy eigenstates of the anharmonic oscillator have to add up to unity.

As we approach the line  $\text{Re } s = 1$  from the right, energy states of larger and larger quantum numbers participate in the time evolution. For this reason our realization of the Riemann  $\zeta$  function is confined to the rather uneventful domain of  $1 < \text{Re } s$  of complex space. In particular, we are not able to build in this way an analog computer which can simulate the Riemann  $\zeta$  function in the critical strip, that is, for  $0 < \text{Re } s < 1$ , where the nontrivial zeros are located.

It is worthwhile to identify the feature which prevents us from conquering this domain. Obviously, we have to satisfy the normalization condition of the quantum state. This requirement is strongly linked to the fact that throughout our article we have taken advantage of the interference property of quantum mechanics. However, we have exclusively concentrated on quantum systems with a single degree of freedom only. In principle, we could have also followed our program for realizing the Riemann  $\zeta$  function using classical light, beam splitters and phase shifters. Here the conservation of intensity prevents us from crossing the line  $\text{Re } s = 1$ .

One possibility [43] for circumventing the normalization requirement is offered by the use of two entangled quantum systems and a joint measurement. This approach is particularly intriguing since then the counterpart of the technique of analytical continuation of complex analysis would be played by the phenomenon of entanglement in quantum mechanics.

Indeed, one of the many seminal contributions of Riemann to the field of analytical number theory was to start from the Dirichlet representation of  $\zeta$  and obtain an analytical continuation of  $\zeta$  to the left of  $\text{Re } s = 1$ . Moreover, according to Erwin Schrödinger, entanglement is *the* trademark of quantum mechanics. Unfortunately, the answer to the question of how to connect these two topics central to quantum physics and complex analysis goes beyond the scope of the present article. It suffices to say that in a forthcoming article [27] we interpret the Riemann-Siegel formula of the Riemann  $\zeta$  function as a superposition of two quantum states with opposite phases. For the harmonic oscillator, such Schrödinger cat states [44] have been realized in cavity QED [45] and ion trap [46] experiments using entanglement and joint measurements. It is fascinating to translate this well-established formalism to the thermal phase states which are at the very heart of the Riemann  $\zeta$  function. In this interpretation the nontrivial zeros of  $\zeta$  are a consequence of a Schrödinger cat.

#### ACKNOWLEDGMENTS

We thank V. Buzek, I. J. Cirac, C. Feiler, M. Knauf, E. Lieb, H. Maier, W. Merkel, G. G. Paulus, F. Schmidt-Kaler, J. Twamley, K. Vogel, and S. Wölk for many fruitful discussions on wave-packet dynamics and number theory. One of us (W.P.S.) is grateful to the late J. A. Wheeler for introducing him to semiclassical quantum mechanics and, in particular, to the RKR method. Moreover, we appreciate the support of the Landesstiftung Baden-Württemberg in the framework of the Quantum Information Highway A8 and the Ministerium für Wissenschaft und Kunst, Baden-Württemberg. In addition, H.M.C. and J.P.D. are most grateful to the Alexander von Humboldt-Stiftung. This research was also partially supported by the Max Planck Research program. R.M. thanks the graduate school Mathematical Analysis of Evolution, Information and Complexity for financial support.

#### APPENDIX A: ANALOGY TO JAYNES-CUMMINGS MODEL

Sums of the type given by Eq. (5) are not restricted to mechanical oscillators and to the notion of the autocorrelation function. They also appear in many other quantum systems and then represent different physical quantities.

For example, in the Jaynes-Cummings model [10] describing the interaction of a single mode of the electromagnetic field in a high- $Q$  cavity with a two-level atom the atomic dynamics is governed by the sum

$$\mathcal{S}(t) \equiv \sum_{n=0}^{\infty} W_n e^{-i\omega_n t}, \quad (\text{A1})$$

where  $\omega_n \equiv f(n)g$ . Here  $g$  is the vacuum Rabi frequency and  $W_n$  denotes the photon statistics of the field. The dependence of the function  $f(n)$  can [10] be “engineered.” For a resonant interaction we find  $f(n) = \sqrt{n}$ , whereas in the limit of strong detuning we obtain  $f(n) = n$ .

The experiments with the one-atom maser summarized in Ref. [47] have studied the resonant interaction of the atom with

the cavity field in a thermal state of temperature  $T$  and make use of the thermal photon statistics

$$W_n = W_0 e^{-\sigma n}. \quad (\text{A2})$$

We emphasize that although the time dependence of the atomic population in the Jaynes-Cummings model [Eq. (A1)] is governed by a sum of the type of the autocorrelation [Eq. (5)], it does not originate from the time evolution of a *single* quantum system but of *two* interacting ones. In particular, Eq. (A1) cannot be derived [10] following the approach of Sec. II A.

The fact that *two* quantum systems rather than a *single* one are involved shall play an important role when we extend our ideas of realizing the Riemann  $\zeta$  function  $\zeta = \zeta(s, a)$  into the critical domain [7] of complex space, that for  $\text{Re } s < 1$ . Indeed, as briefly mentioned in Sec. VII and is further detailed in Ref. [27], we take advantage of entanglement of *two* quantum systems to implement the corresponding representation of  $\zeta$  obtained in complex analysis by the method of analytical continuation.

### APPENDIX B: UNIQUENESS OF INVERSE SPECTRAL PROBLEM

In this appendix we briefly recall the central aspects of the elementary Sturm-Liouville problem defined by the differential equation

$$-u_n''(x) + q(x)u_n(x) - \lambda_n u_n(x) = 0. \quad (\text{B1})$$

The operator  $\hat{L}$ ,

$$\hat{L}[u] \equiv -u'' + qu, \quad (\text{B2})$$

is Hermitian on the interval  $b < x < d$  with the boundary conditions

$$\varepsilon u(b) + \beta u'(b) = 0 \quad (\text{B3})$$

and

$$\nu u(d) + \delta u'(d) = 0. \quad (\text{B4})$$

The time-independent Schrödinger equation

$$\frac{d^2}{dx^2} \psi_n(x) + \frac{2\mu}{\hbar^2} [E_n - V(x)] \psi_n(x) = 0 \quad (\text{B5})$$

defines such a Sturm-Liouville problem, with  $\beta = \delta = 0$  (Dirichlet boundary conditions).

The Sturm-Liouville problem has a direct spectral problem and an inverse spectral problem associated with it. The direct problem consists of determining the eigenvalue spectrum  $\lambda_0 < \lambda_1 < \lambda_2 \dots$  for a given  $q(x)$ . In the case of the Schrödinger equation this becomes the problem of determining the energies  $E_0 < E_1 < E_2 \dots$  for a given potential  $V(x)$ . The inverse problem consists of determining the operator  $\hat{L}$  from the eigenvalue spectrum. The direct problem is thoroughly discussed in almost any textbook in quantum mechanics. Interest in the inverse problem has been more modest, but it has been steadily increasing and is now developing rapidly [48].

A fairly comprehensive discussion of the inverse problem was given by the Swedish mathematician Göran Borg in 1946 [49]. He proved that, in general, two sets of eigenvalues

for different boundary conditions uniquely determine the potential  $q(x)$ . For a case like that of Eq. (B5), with the simple Dirichlet boundary conditions, a symmetric potential  $V(x)$  is uniquely defined by all eigenvalues  $E_n$ . Many others [50–53] considerably improved and generalized these results.

In scattering theory this solution, known as the Borg-Marchenko theorem, plays an important role [54] in determining the potential of the half-line Schrödinger operator. All proofs have in common that they rely on local potentials which fulfill the inequality

$$\int_b^d x |q(x)| dx < \infty. \quad (\text{B6})$$

However, we face the inverse spectral problem with an infinite potential. A proof of its uniqueness is not known to us and would probably exceed the topic of this article.

### APPENDIX C: INVERSE SPECTRAL PROBLEM IN JWKB

In this appendix we summarize the essential ingredients of the RKR method in JWKB. Here we consider the quantum motion of a particle of mass  $\mu$  in a one-dimensional potential  $V = V(x)$  and determine  $V$  such that a prescribed discrete energy spectrum  $E_n$  emerges. Expressions similar to ours have been derived in Refs. [55,56]. However, we emphasize that these authors have put the value  $V_0$  of the minimum of  $V$  equal to zero. In our treatment we tie  $V_0$  to the phase change of the JWKB-wave function for the energy  $E = V_0$ . Moreover, we illustrate the RKR technique using the example of the harmonic oscillator.

#### A. From potential to energy spectrum

For simplicity, we consider a potential with a single minimum. We choose the origin of the coordinate axis to be at this minimum, that is,  $V(0) \equiv V_0$ .

The quantity central to our considerations is the phase change

$$F(E) \equiv \sqrt{\frac{2\mu}{\hbar^2}} \int_{x_1(E)}^{x_2(E)} dx \sqrt{E - V(x)} \quad (\text{C1})$$

of the JWKB-wave function corresponding to the classical motion of energy  $E$  caught between the two turning points  $x_1(E) < x_2(E)$ .

Our goal is to replace the integration variable  $x$  in Eq. (C1) with the potential  $V(x) \equiv E'$ . For this purpose we have to decompose the integration region into domains where  $V(x)$  is monotonous, that is,  $x_1 \leq x \leq 0$  and  $0 \leq x \leq x_2$ . The limits of the first integration then correspond to  $E$  and  $V_0$ , whereas in the second integral they are  $V_0$  and  $E$ , giving rise to the integral

$$F(E) = \sqrt{\frac{2\mu}{\hbar^2}} \int_{V_0}^E dE' \sqrt{E - E'} \left[ \frac{dx_2(E')}{dE'} - \frac{dx_1(E')}{dE'} \right]. \quad (\text{C2})$$

When we introduce the excursion

$$X(E) \equiv x_2(E) - x_1(E) \quad (\text{C3})$$

of the classical motion corresponding to the energy  $E$ , we find

$$F(E) = \sqrt{\frac{2\mu}{\hbar^2}} \int_{V_0}^E dE' \sqrt{E - E'} \frac{dX}{dE'}, \quad (\text{C4})$$

which after partial integration takes the form

$$F(E) = \sqrt{\frac{2\mu}{\hbar^2}} [X(E') \sqrt{E - E'}]_{V_0}^E + \sqrt{\frac{2\mu}{\hbar^2}} \int_{V_0}^E dE' \frac{X(E')}{2\sqrt{E - E'}}. \quad (\text{C5})$$

At the minimum of the potential, that is, at  $x = 0$ , the excursion vanishes, that is,

$$X(V_0) = 0. \quad (\text{C6})$$

As a result, the boundary term in Eq. (C5) due to the lower limit  $E' = V_0$  vanishes. Likewise, the upper part is zero due to the square root.

Hence, the phase change is solely expressed by the integral

$$F(E) = \sqrt{\frac{\mu}{2\hbar^2}} \int_{V_0}^E dE' \frac{X(E')}{\sqrt{E - E'}} \quad (\text{C7})$$

over the excursion.

We note that at the minimum of the potential the phase change vanishes, that is,

$$F(V_0) = 0. \quad (\text{C8})$$

Quantization is obtained by the familiar JWKB condition [4]

$$F(E_n) = \pi(n + \alpha), \quad n = 0, 1, 2, \dots \quad (\text{C9})$$

on the phase change where  $\alpha$  is the Maslov index [26].

The allowed energies  $E_n$  are finally obtained by inverting the function  $n = n(E)$  given by Eq. (C9).

### B. From energy spectrum to potential

In the preceding section we have started from a given potential  $V$  and have expressed the phase change  $F(E)$  in terms of the excursion  $X$  and a square root of the energy. When we quantize  $F(E)$  and invert this relation, we obtain the quantized energies  $E_n$ .

We now follow this path in the opposite direction. Indeed, we start from the energy spectrum, that is, we know  $E_n$  and find the potential by inverting the expression [Eq. (C7)] for the phase change  $F$  to obtain the excursion  $X$ .

Collocating the  $n$  values allows us to construct a continuous function  $n = n(E)$ , which when inserted into the expression (C9) gives us the phase change  $F(E)$ , that is,

$$\pi[n(E) + \alpha] = F(E) \quad (\text{C10})$$

or

$$\pi[n(E) + \alpha] = \sqrt{\frac{\mu}{2\hbar^2}} \int_{V_0}^E dE' \frac{X(E')}{\sqrt{E - E'}}. \quad (\text{C11})$$

Here we have made use of the expression [Eq. (C7)] for  $F$ .

The left-hand side of Eq. (C11) is known. We now need to search for the excursion  $X(E)$  which appears in the integral on the right-hand side. Consequently, Eq. (C11) represents an integral equation, which is of the Abel type [57,58].

In Appendix D we briefly review a method of inverting the Abel integral equation and derive the expression

$$X(E) = \sqrt{\frac{2\hbar^2}{\mu}} \int_{V_0}^E dE' \frac{1}{\sqrt{E - E'}} \frac{dn(E')}{dE'} \quad (\text{C12})$$

for the excursion. However, for the present discussion it suffices to show that Eq. (C12) is a solution of Eq. (C11).

For this purpose we substitute Eq. (C12) into the right-hand side of Eq. (C11) and find the integral

$$I \equiv \int_{V_0}^E dE' \frac{1}{\sqrt{E - E'}} \int_{V_0}^{E'} dE'' \frac{1}{\sqrt{E' - E''}} \frac{dn(E'')}{dE''}, \quad (\text{C13})$$

which after interchanging the order of integrations yields

$$I = \int_{V_0}^E dE'' \frac{dn(E'')}{dE''} \int_{E''}^E dE' \frac{1}{\sqrt{E - E'} \sqrt{E' - E''}}. \quad (\text{C14})$$

With the help of the substitution

$$y \equiv \frac{2E'}{E - E''} - \frac{E + E''}{E - E''}, \quad (\text{C15})$$

the integral over  $E'$  can be performed and yields

$$\int_{E''}^E dE' \frac{1}{\sqrt{E - E'} \sqrt{E' - E''}} = \int_{-1}^1 dy \frac{1}{\sqrt{1 - y^2}} = \pi. \quad (\text{C16})$$

As a consequence, we arrive at

$$I = \pi \int_{V_0}^E dE'' \frac{dn(E'')}{dE''} = \pi[n(E) - n(V_0)]. \quad (\text{C17})$$

The condition Eq. (C8) on the phase change to vanish at the bottom of the potential creates a relation between  $n(V_0)$  and the Maslov index  $\alpha$ . Indeed, we find from Eq. (C10), with the help of Eq. (C8), the identity

$$n(V_0) + \alpha = 0. \quad (\text{C18})$$

When we substitute this result into Eq. (C17), we arrive at the left-hand side of Eq. (C11). As a result, the excursion given by Eq. (C12) is the potential.

Needless to say, the so-constructed potential leads via the JWKB quantization to the energy spectrum we have started from. Moreover, we emphasize that in this derivation we have neglected the implicit uncertainty in the function  $F(E)$  due to making  $n(E)$  a continuous function.

### C. Example: Harmonic oscillator

Next we illustrate the RKR method summarized by the expression for the excursion [Eq. (C12)], together with the supplementary condition [Eq. (C18)] with the example of an equidistant energy spectrum,

$$E_n^{(\text{os})} \equiv \hbar\omega(n + \frac{1}{2}), \quad (\text{C19})$$

corresponding to the harmonic oscillator.

When we invert the spectral relation [Eq. (C19)], we find

$$n(E) = \frac{E}{\hbar\omega} - \frac{1}{2}, \quad (\text{C20})$$

which, together with Eq. (C12), yields the excursion

$$X(E) = 2\left(\frac{1}{2}\mu\omega^2\right)^{-1/2}\sqrt{E - V_0} \quad (\text{C21})$$

and the potential

$$V(x; V_0) = V_0 + \frac{1}{2}\mu\omega^2 x^2. \quad (\text{C22})$$

This potential creates the energy spectrum

$$E_n = V_0 + \hbar\omega(n + \alpha). \quad (\text{C23})$$

In order to be consistent with the energy spectrum (C19) we have started from, we need  $V_0 = 0$  and  $\alpha = 1/2$ . For this purpose we first recall [21] that the Maslov index  $\alpha$  of a potential with two turning points each providing a contribution  $+1/4$  is given by  $\alpha = 1/2$ . Hence, we find from the supplementary condition [Eq. (C18)] with the help of Eq. (C20) the identity

$$\frac{V_0}{\hbar\omega} - \frac{1}{2} + \frac{1}{2} = 0, \quad (\text{C24})$$

which implies  $V_0 = 0$ .

#### APPENDIX D: ABEL INTEGRAL TRANSFORM

In this appendix we briefly review the derivation of the Abel integral transform and obtain two equivalent representations. Moreover, we apply these results to rederive the expression Eq. (C12) for the excursion.

##### A. General method

We consider the equation

$$f(E') = \int_{V_0}^{E'} dE'' \frac{g(E'')}{\sqrt{E' - E''}}, \quad (\text{D1})$$

with the goal to express the function  $g = g(E)$  in terms of the function  $f = f(E)$ .

For this purpose we multiply both sides of Eq. (D1) by  $\pi^{-1}(E - E')^{-1/2}$  and integrate over  $E'$  from  $V_0$  to  $E$ , which results in

$$\begin{aligned} & \frac{1}{\pi} \int_{V_0}^E dE' \frac{f(E')}{\sqrt{E - E'}} \\ &= \frac{1}{\pi} \int_{V_0}^E dE' \frac{1}{\sqrt{E - E'}} \int_{V_0}^{E'} dE'' \frac{g(E'')}{\sqrt{E' - E''}} \equiv I. \end{aligned} \quad (\text{D2})$$

Next we interchange the order of the integrations in the double integral and arrive at

$$I = \int_{V_0}^E dE'' g(E'') \frac{1}{\pi} \int_{E''}^E dE' \frac{1}{\sqrt{E - E'}\sqrt{E' - E''}}, \quad (\text{D3})$$

which with the help of the integral formula [Eq. (C16)] leads to

$$I = \int_{V_0}^E dE'' g(E''). \quad (\text{D4})$$

As a consequence, Eq. (D2) reduces to

$$\frac{1}{\pi} \int_{V_0}^E dE' \frac{f(E')}{\sqrt{E - E'}} = \int_{V_0}^E dE'' g(E''). \quad (\text{D5})$$

When we differentiate both sides with respect to  $E$ , we find

$$g(E) = \frac{1}{\pi} \frac{d}{dE} \left[ \int_{V_0}^E dE' \frac{f(E')}{\sqrt{E - E'}} \right] \equiv \frac{1}{\pi} \frac{d}{dE} J(E). \quad (\text{D6})$$

We emphasize that we have to differentiate  $J(E)$  with respect to the variable  $E$  which appears in the upper limit of the integration as well as in the square root underneath the integral. These differentiations lead to divergent expressions. Therefore, it is useful to first integrate by parts before performing the differentiation; that is,

$$J(E) = -2\sqrt{E - E'} f(E')|_{V_0}^E + 2 \int_{V_0}^E dE' \sqrt{E - E'} \frac{df(E')}{dE'}. \quad (\text{D7})$$

The boundary term simplifies since at the upper limit the square root vanishes. As a result we find the identity

$$J(E) = 2\sqrt{E - V_0} f(V_0) + 2 \int_{V_0}^E dE' \sqrt{E - E'} \frac{df(E')}{dE'}. \quad (\text{D8})$$

Now we differentiate with respect to  $E$  and note that the dependence of the upper limit of the integral does not contribute due to the vanishing of the square root, which leads us to

$$g(E) = \frac{1}{\pi} \left[ \frac{f(V_0)}{\sqrt{E - V_0}} + \int_{V_0}^E dE' \frac{1}{\sqrt{E - E'}} \frac{df(E')}{dE'} \right]. \quad (\text{D9})$$

This expression is completely equivalent to the one in Eq. (D6).

##### B. Application to excursion

Next we apply Eq. (D9) to rederive the expression Eq. (C12) for the excursion using the Abel integral equation

$$\pi[n(E) + \alpha] = \sqrt{\frac{\mu}{2\hbar^2}} \int_{V_0}^E dE' \frac{X(E)}{\sqrt{E - E'}}. \quad (\text{D10})$$

A comparison with Eq. (D1) immediately provides us with the identifications  $f \equiv \pi[n(E) + \alpha]$  and  $g \equiv X\sqrt{\mu/(2\hbar^2)}$ , which when substituted into Eq. (D9) yields

$$X(E) = \sqrt{\frac{2\hbar^2}{\mu}} \left[ \frac{n(V_0) + \alpha}{\sqrt{E - V_0}} + \int_{V_0}^E dE' \frac{1}{\sqrt{E - E'}} \frac{dn(E')}{dE'} \right]. \quad (\text{D11})$$

With the help of the supplementary condition Eq. (C18), we arrive indeed at Eq. (C12).

#### APPENDIX E: MORE ON LOGARITHMIC POTENTIALS

In Sec. IV we compare and contrast the JWKB energy eigenvalues of a purely logarithmic potential to the exact ones obtained by a numerical method. This discussion is motivated by the problem of obtaining the potential which provides us with a logarithmic energy spectrum. However, the purely logarithmic potential

$$U(x) = U_0 \ln\left(\frac{x}{b}\right) \quad (\text{E1})$$

leads to many unusual features that make it interesting to study it independent of the inverse spectral problem. We dedicate the present appendix to highlight some of these properties. Throughout this appendix we restrict the coordinate  $x$  to positive values, that is,  $0 \leq x < \infty$ . Moreover,  $U_0 \equiv \hbar\omega$  denotes the strength of the potential and  $b$  is a chosen characteristic length.

### A. Average kinetic energy is independent of mass

The virial theorem [4] states that twice the expectation value  $\langle \hat{p}^2 / (2\mu) \rangle$  of the kinetic energy operator is identical to the expectation value  $\langle \hat{x} \frac{dV(\hat{x})}{dx} \rangle$  of the product of the operators of the position  $\hat{x}$  and the derivative of the potential  $\hat{V} = V(\hat{x})$ , that is,

$$2 \left\langle \frac{\hat{p}^2}{2\mu} \right\rangle = \left\langle \hat{x} \frac{d\hat{V}}{dx} \right\rangle. \quad (\text{E2})$$

For a potential of the form  $V(x) = Ax^n$ , where  $A$  is a constant, the virial theorem predicts

$$2 \left\langle \frac{\hat{p}^2}{2\mu} \right\rangle = n \langle \hat{V} \rangle. \quad (\text{E3})$$

However, for the logarithmic potential  $U$  defined by Eq. (E1) we get

$$2 \left\langle \frac{\hat{p}^2}{2\mu} \right\rangle = U_0. \quad (\text{E4})$$

Thus, the expectation value of the kinetic energy is the same for all stationary states. It is also independent of the mass of the particle. This is a remarkable result.

### B. Level spacing is independent of mass

The unusual feature Eq. (E4) has its origin in a scaling property of the Schrödinger equation

$$\left[ \frac{\hbar^2}{2\mu} \frac{d^2}{dx^2} + E(\mu) - U_0 \ln \left( \frac{x}{b} \right) \right] u(x) = 0 \quad (\text{E5})$$

in the mass  $\mu$  unique to the logarithmic potential. For the present discussion it is useful to indicate the mass dependence of the energy eigenvalue  $E = E(\mu)$ .

For a different mass  $\mu'$  the Schrödinger equation

$$\left[ \frac{\hbar^2}{2\mu'} \frac{d^2}{dy^2} + E(\mu') - U_0 \ln \left( \frac{y}{b} \right) \right] v(y) = 0 \quad (\text{E6})$$

for the eigenfunctions  $v = v(y)$  with energy eigenvalues  $E(\mu')$  is connected to one with mass  $\mu$  by the scaling transformation

$$x \equiv \sqrt{\frac{\mu'}{\mu}} y \quad (\text{E7})$$

of the coordinates.

The functional relation

$$\ln \frac{x}{b} \equiv \ln \left( \sqrt{\frac{\mu'}{\mu}} \frac{y}{b} \right) = \frac{1}{2} \ln \frac{\mu'}{\mu} + \ln \frac{y}{b} \quad (\text{E8})$$

of the logarithm yields the identification

$$v(y) \equiv u \left( \sqrt{\frac{\mu'}{\mu}} y \right) \quad (\text{E9})$$

and the connection formula

$$E(\mu') = E(\mu) - \frac{1}{2} U_0 \ln \left( \frac{\mu'}{\mu} \right) \quad (\text{E10})$$

of the energies  $E(\mu')$  and  $E(\mu)$  corresponding to the masses  $\mu'$  and  $\mu$ , respectively.

Since Eq. (E10) must hold for any pair of corresponding energy levels, the energy difference between the  $i$ th and the  $j$ th level reads

$$E_i(\mu') - E_j(\mu') = E_i(\mu) - E_j(\mu). \quad (\text{E11})$$

Hence, the level spacing is independent of the mass.

### C. From potential to energy levels

Next we verify that within the JWKB approximation the purely logarithmic potential  $U = U(x)$  given by Eq. (E1) indeed leads to a logarithmic energy spectrum. Obviously, this fact is guaranteed by the uniqueness of the Abel transform. Nevertheless, it is instructive to perform the relevant steps of the calculation since in this way we can connect the parameters of the motion of a particle in a potential such as mass with the parameters of the energy spectrum.

We substitute the excursion

$$X(E) = be^{E/U_0} \quad (\text{E12})$$

for the purely logarithmic potential given by Eq. (E1) into Eq. (C7) for the phase change  $F = F(E)$  and find

$$F(E) = \sqrt{\frac{\mu}{2\hbar^2}} b \int_{-\infty}^E dE' \frac{e^{E'/U_0}}{\sqrt{E - E'}}. \quad (\text{E13})$$

Here we have also recalled that  $V_0 = -\infty$  for the purely logarithmic potential.

With the help of the new integration variable

$$\eta \equiv -\frac{E'}{E}, \quad (\text{E14})$$

Eq. (E13) takes the form

$$F(E) = \sqrt{\frac{\mu}{2\hbar^2}} b \sqrt{E} \int_{-1}^{\infty} d\eta \frac{\exp(-\frac{E}{U_0} \eta)}{\sqrt{1 + \eta}}, \quad (\text{E15})$$

which reduces with the integral formula [59]

$$\int_{-1}^{\infty} d\eta \frac{e^{-q\eta}}{\sqrt{1 + \eta}} = e^q \sqrt{\frac{\pi}{q}} \quad (\text{E16})$$

valid for  $0 < q$  to

$$F(E) = \sqrt{\frac{\mu}{2\hbar^2}} b \sqrt{\pi U_0} e^{E/U_0}. \quad (\text{E17})$$

The quantization condition Eq. (C9) finally yields

$$E_n = U_0 \ln \left[ \sqrt{\frac{2\pi\hbar^2}{\mu b^2 U_0}} (n + \alpha) \right]. \quad (\text{E18})$$

When we compare this expression for the JWKB energy in the purely logarithmic potential to the desired energy spectrum Eq. (1), we can make the identifications

$$a = \alpha \quad (\text{E19})$$

and

$$\gamma \equiv \sqrt{\frac{2\pi\hbar^2}{\mu b^2 U_0}}. \quad (\text{E20})$$

It is worth mentioning that the identity [Eq. (E19)] between the Hurwitz parameter  $a$  and the Maslov index  $\alpha$  also follows from Eq. (39) in the limit of  $V_0 \rightarrow -\infty$ . Since Eq. (E20) implies the scaling law

$$\gamma(\mu') = \sqrt{\frac{\mu}{\mu'}} \gamma(\mu), \quad (\text{E21})$$

we find from Eq. (E18) the mass dependence

$$E_n(\mu') = E_n(\mu) + \frac{1}{2} U_0 \ln\left(\frac{\mu}{\mu'}\right) = E_n(\mu) - \frac{1}{2} U_0 \ln\left(\frac{\mu'}{\mu}\right) \quad (\text{E22})$$

of the JWKB energy eigenvalues  $E_n$  in complete agreement with the scaling law [Eq. (E10)] following from the Schrödinger equation [Eq. (E5)].

#### D. Uniqueness

One might wonder if the remarkable dependence of the energy on the mass of the particle expressed by Eq. (E10) is unique to the purely logarithmic potential. Indeed, we can trace this property back to the functional relation

$$\ln(c_1 c_2) = \ln c_1 + \ln c_2 \quad (\text{E23})$$

of the logarithm, which has allowed us to obtain the decomposition [Eq. (E8)] of the mass contributions. Since Eq. (E23) defines the logarithmic function uniquely, we must conclude that the purely logarithmic potential  $U = U(x)$  defined by Eq. (E1) is the only potential giving rise to the energy-mass scaling of Eq. (E10).

It is interesting to note that Eq. (39), which connects  $V_0$  to  $\gamma$ ,  $a$ , and  $\alpha$  ensures that the energy in the potential  $V$  implicitly defined by Eq. (41), does not satisfy the scaling property [Eq. (E10)]. We recall that the RKR method constructs this potential within the JWKB approximation such that the emerging energy spectrum is given by the desired logarithmic eigenvalue distribution [Eq. (1)]. However, at this point it is not clear how the mass of the particle makes its appearance in Eq. (1).

Since the parameter  $\kappa$  [Eq. (32)] is proportional to the square root of the mass, we find the scaling relation

$$\kappa(\mu') = \sqrt{\frac{\mu'}{\mu}} \kappa(\mu). \quad (\text{E24})$$

In Eq. (41) the parameter  $\kappa$  appears only on the left-hand side of the equation in a product with  $\gamma$ . It is therefore tempting to redefine  $\gamma$  in the way suggested by Eq. (E21). However, due to the constraint Eq. (39), the parameter  $\gamma$  also appears on the right-hand side of Eq. (41) and prevents in this way the rescaling of the equation for the potential. Only in the limit

of  $V_0 \rightarrow -\infty$  do we achieve the scaling property [Eq. (E10)], since in this case the right-hand side of Eq. (41) is independent of  $\gamma$ .

#### E. From one to three dimensions: Quarkonium

In three dimensions the potential as well as the Schrödinger equation [Eqs. (E1) and (E5)] are replaced by

$$U(r) = U_0 \ln\left(\frac{r}{b}\right), \quad (\text{E25})$$

with  $0 < r < \infty$  and

$$\left[ \frac{\hbar^2}{2\mu} \frac{d^2}{dr^2} + E - \frac{\hbar^2 \ell(\ell+1)}{2\mu r^2} - U_0 \ln\left(\frac{r}{b}\right) \right] u(r) = 0. \quad (\text{E26})$$

Here  $r \equiv \sqrt{x^2 + y^2 + z^2}$  and  $\ell$  denote the radial variable and the angular momentum quantum number, respectively, and  $u = u(r)$  is the reduced radial function. For  $s$  states, where  $\ell = 0$ , Eqs. (E5) and (E26) become formally identical.

With  $r$  being the distance between two particles interacting through central forces and  $\mu$  being the reduced mass of the two particles, Eq. (E26) may be interpreted as the radial Schrödinger equation for the relative motion of two such particles. The preceding findings about kinetic energy and level spacings remain valid in three dimensions. They are in harmony with the experimentally found properties of quarkonium, which is built from a quark and an antiquark. The logarithmic potential has accordingly been considered a possible candidate for the interaction potential in this composite particle [60].

This application has stimulated the interest in Eq. (E26) and its solutions. Some authors have presented numerical solutions of Eq. (E26) for several values of  $\ell$  and the radial quantum number  $n$ . A nonexhaustive list includes work using the shifted  $1/N$  expansion [61], the standard variation technique [62], and a generalized pseudospectral method [63]. Especially noteworthy is in this case the approach of Refs. [64,65] based on a perturbation expansion.

#### F. Two dimensions: A hydrogen-atom model

In two dimensions the logarithmic potential reads

$$U(\rho) = U_0 \ln\left(\frac{\rho}{a}\right), \quad 0 < \rho < \infty, \quad (\text{E27})$$

and is thus identical to Eq. (E25), but with  $\rho \equiv \sqrt{x^2 + y^2}$ . Moreover, the radial Schrödinger equation becomes

$$\left[ \frac{\hbar^2}{2\mu} \frac{d^2}{d\rho^2} + E - \frac{\hbar^2(m^2 - 1/4)}{2\mu\rho^2} - U_0 \ln\left(\frac{\rho}{a}\right) \right] u(\rho) = 0, \quad (\text{E28})$$

where  $u = u(\rho)$  denotes the radial wave function and  $m$  is the angular-momentum quantum number. Because of the so-called anticentrifugal potential  $-\hbar^2/8\mu\rho^2$  [66], Eq. (E28) is formally different from Eq. (E5) for  $m = 0$ .

Equation (E28) has attracted some attention in the literature as a possible radial Schrödinger equation for a two-dimensional hydrogen atom, and solutions have been obtained for several levels, by means of the variational method [67,68].

The structure of the three-dimensional hydrogen atom is, of course, determined by the well-known Coulomb potential, and that potential has also been used in the description of a hypothetical two-dimensional hydrogen atom. It has, however, been argued that the potential should be chosen with reference to Gauss' theorem. In three dimensions, this theorem is satisfied by the Coulomb potential, and in two dimensions by the logarithmic potential. This is the rationale behind the interest in the two-dimensional logarithmic potential.

#### APPENDIX F: EIGENVALUE CORRECTIONS

In Sec. III we have found a potential which in JWKB approximation provides us with a logarithmic energy spectrum. However, when we solve in Sec. IV the Schrödinger equation in the presence of this potential in an exact way we do not arrive at this predescribed spectrum. Therefore, we need to obtain an improved potential using perturbation theory as well as an iteration algorithm. In the present appendix we briefly summarize the perturbative approach, which is based on the Hellmann-Feynman theorem [23–25].

We consider the Hamiltonian

$$\hat{H}_\beta \equiv \hat{H}^{(0)} + \delta V(\hat{x}; \boldsymbol{\beta}), \quad (\text{F1})$$

consisting of the Hamiltonian

$$\hat{H}^{(0)} = \frac{\hat{p}^2}{2\mu} + V^{(0)}(\hat{x}), \quad (\text{F2})$$

with the potential  $V^{(0)}(\hat{x})$  obtained by the RKR method discussed in Appendix C and a small correction potential  $\delta V(x; \boldsymbol{\beta})$ . Here the vector  $\boldsymbol{\beta}$  consists of the components  $\beta_n$ , which describe the shape of the correction. For  $\boldsymbol{\beta} \rightarrow 0$  the correction potential vanishes.

The states  $|\varphi_m\rangle$  satisfy the energy eigenvalue equation

$$\hat{H}_\beta |\varphi_m\rangle = E_m |\varphi_m\rangle, \quad (\text{F3})$$

where the energies  $E_m$  and the eigenstates  $|\varphi_m\rangle$  depend on  $\boldsymbol{\beta}$ .

We can express  $E_m$  with a Taylor series

$$E_m = E_m|_{\boldsymbol{\beta}=0} + \sum_n \left. \frac{\partial E_m}{\partial \beta_n} \right|_{\boldsymbol{\beta}=0} \beta_n + O(\boldsymbol{\beta}^2) \quad (\text{F4})$$

around  $\boldsymbol{\beta} = 0$ .

The energies  $E_m$  at  $\boldsymbol{\beta} = 0$  are the eigenvalues  $E_m^{(0)}$  of the Hamiltonian  $\hat{H}_0$ . Moreover, we obtain the derivatives of

$E_m$  with respect to the parameters  $\beta_n$  by differentiating the definition

$$E_m \equiv \langle \varphi_m | \hat{H}_\beta | \varphi_m \rangle, \quad (\text{F5})$$

which yields

$$\begin{aligned} \frac{\partial E_m}{\partial \beta_n} = & \left( \frac{\partial}{\partial \beta_n} \langle \varphi_m | \right) \hat{H}_\beta | \varphi_m \rangle + \langle \varphi_m | \left( \frac{\partial}{\partial \beta_n} \hat{H}_\beta \right) | \varphi_m \rangle \\ & + \langle \varphi_m | \hat{H}_\beta \left( \frac{\partial}{\partial \beta_n} | \varphi_m \rangle \right). \end{aligned} \quad (\text{F6})$$

The eigenvalue equation (F3) allows us to combine the first and the third term in Eq. (F6) as the derivative of the state vector with respect to  $\beta_n$ . According to Eq. (F1) the differentiation of  $\hat{H}_\beta$  with respect to  $\beta_n$  only includes the potential  $\delta V$ , which leads us to

$$\frac{\partial E_m}{\partial \beta_n} = E_m \frac{\partial}{\partial \beta_n} \langle \varphi_m | \varphi_m \rangle + \langle \varphi_m | \left( \frac{\partial}{\partial \beta_n} \delta V(\hat{x}; \boldsymbol{\beta}) \right) | \varphi_m \rangle. \quad (\text{F7})$$

When we assume that the eigenstates  $|\varphi_m\rangle$  are normalized, Eq. (F7) reads

$$\frac{\partial E_m}{\partial \beta_n} = \langle \varphi_m | \left( \frac{\partial}{\partial \beta_n} \delta V(\hat{x}; \boldsymbol{\beta}) \right) | \varphi_m \rangle. \quad (\text{F8})$$

In the limit of  $\boldsymbol{\beta} = 0$  this expression reduces to

$$\left. \frac{\partial E_m}{\partial \beta_n} \right|_{\boldsymbol{\beta}=0} = \langle \varphi_m^{(0)} | \left. \frac{\partial}{\partial \beta_n} \delta V(\hat{x}; \boldsymbol{\beta}) \right|_{\boldsymbol{\beta}=0} | \varphi_m^{(0)} \rangle, \quad (\text{F9})$$

where  $|\varphi_m^{(0)}\rangle$  denote the energy eigenstates of the unperturbed Hamiltonian  $\hat{H}^{(0)}$  with energy eigenvalue  $E_m^{(0)}$ .

When we substitute the expression for the first derivative of  $E_m$  with respect to  $\beta_n$  given by Eq. (F9) into the Taylor series (F4), we arrive at the linear system of equations

$$\sum_n M_{mn} \beta_n = E_m - E_m^{(0)} \quad (\text{F10})$$

for the parameters  $\beta_n$  with the matrix

$$M_{mn} \equiv \langle \varphi_m^{(0)} | \left. \frac{\partial}{\partial \beta_n} \delta V(\hat{x}; \boldsymbol{\beta}) \right|_{\boldsymbol{\beta}=0} | \varphi_m^{(0)} \rangle. \quad (\text{F11})$$

Hence, we have derived a matrix equation in which the variation of the energies  $E_n - E_n^{(0)}$  determines the parameters  $\boldsymbol{\beta}$  of the correction potential  $\delta V(x; \boldsymbol{\beta})$ .

[1] S. Stenholm and K.-A. Suominen, *Quantum Approach to Informatics* (Wiley, New York, 2005).  
 [2] D. Bouwmeester, A. Ekert, and A. Zeilinger, *The Physics of Quantum Information* (Springer-Verlag, Berlin, 2001).  
 [3] J. P. Keating, in *Quantum Chaos*, edited by G. Casati, I. Guarneri, and U. Smilansky (North-Holland, Amsterdam, 1993).  
 [4] See, for instance, E. Merzbacher, *Quantum Mechanics* (Wiley, New York, 1961).  
 [5] See, for example, H. Davenport, *Multiplicative Number Theory* (Springer-Verlag, New York, 2000).  
 [6] See, for example, D. J. Tannor, *Introduction to Quantum Mechanics: A Time-Dependent Perspective* (University Science Books, Sausalito, 2006).

[7] H. Maier and W. P. Schleich, *Prime Numbers 101, A Primer on Number Theory* (Wiley, New York, 2010).  
 [8] J. H. Shapiro, S. R. Shepard, and N. Wong, *Phys. Rev. A* **43**, 3795 (1991).  
 [9] E. T. Whittaker and G. N. Watson, *A Course of Modern Analysis*, 4th ed. (Cambridge University Press, Cambridge, UK, 1963).  
 [10] See, for example, W. P. Schleich, *Quantum Optics in Phase Space* (Wiley-VCH, Berlin, 2001).  
 [11] V. Lethokhov, *Laser Control of Atoms and Molecules* (Oxford University Press, Oxford, UK, 2007).  
 [12] T. Fuji, J. Rauschenberger, Ch. Gohle, A. Apolonski, Th. Udem, V. S. Yakovlev, G. Tempea, T. W. Hänsch, and F. Krausz, *New J. Phys.* **7**, 1 (2005).

- [13] W. Paul, *Rev. Mod. Phys.* **62**, 531 (1990).
- [14] H. Walther, *Fortschr. Phys.* **54**, 617 (2006).
- [15] See, for example, J. Wals, H. H. Fielding, J. F. Christian, L. C. Snoek, W. J. van der Zande, and H. B. van Linden van den Heuvell, *Phys. Rev. Lett.* **72**, 3783 (1994).
- [16] D. M. Meekhof, C. Monroe, B. E. King, W. M. Itano, and D. J. Wineland, *Phys. Rev. Lett.* **76**, 1796 (1996).
- [17] M. Morinaga, I. Bouchoule, J.-C. Karam, and C. Salomon, *Phys. Rev. Lett.* **83**, 4037 (1999).
- [18] M. J. J. Vrakking, D. M. Villeneuve, and A. Stolow, *Phys. Rev. A* **54**, R37 (1996).
- [19] K. Chadan, D. Colton, L. Päivärinta, and W. Rundell, *An Introduction to Inverse Scattering and Inverse Spectral Problems* (SIAM, Philadelphia, 1997).
- [20] R. Rydberg, *Z. Phys.* **73**, 376 (1931); **80**, 514 (1933); O. Klein, *ibid.* **76**, 226 (1932); A. L. G. Rees, *Proc. Phys. Soc.* **59**, 998 (1947).
- [21] J. A. Wheeler, in *Studies in Mathematical Physics, Essays in Honor of Valentine Bargmann*, edited by E. H. Lieb, B. Simon, and A. S. Wightman (Princeton University Press, Princeton, 1976).
- [22] M. S. Child, *Semiclassical Mechanics with Molecular Applications* (Clarendon Press, Oxford, UK, 1991).
- [23] H. Hellmann, *Einführung in die Quantenchemie* (Franz Deuticke, Leipzig, 1937), p. 285.
- [24] R. P. Feynman, *Phys. Rev.* **56**, 340 (1939).
- [25] Today this type of perturbation theory runs by the name of Hellmann-Feynman theorem. However, it is interesting that it was already mentioned in earlier works, for example, by P. Güttinger, *Z. Phys.* **73**, 169 (1932), and W. Pauli, *Handbuch der Physik* (Springer, Berlin, 1933), p. 162.
- [26] V. P. Maslov and M. V. Fedoriuk, *Semiclassical Approximation in Quantum Mechanics* (Reidel, Dordrecht, 1981).
- [27] C. Feiler, R. Mack, and W. P. Schleich (unpublished).
- [28] See, for example, W. Rundell in Ref. [19].
- [29] See, for example, B. Däubler, Ch. Miller, H. Risken, and L. Schönörf, *Phys. Scr. T* **48**, 119 (1993), and references therein.
- [30] H. Friedrich and J. Trost, *Phys. Rev. Lett.* **76**, 4869 (1996).
- [31] See, for example, J. Stoer and R. Bulirsch, *Introduction to Numerical Analysis* (Springer, Heidelberg, 1992); J. L. M. Quiroz Gonzalez and D. Thompson, *Comput. Phys.* **11**, 514 (1997).
- [32] J. P. Dahl, *J. Phys. Chem.* **99**, 2727 (1995).
- [33] R. E. Langer, *Phys. Rev.* **51**, 669 (1937); see also, J. P. Dahl and W. P. Schleich, *J. Phys. Chem. A* **108**, 8713 (2004).
- [34] D. Spector, *J. Phys. A* **37**, 4861 (2004).
- [35] U. Drodofsky, J. Stuhler, T. Schulze, M. Drewsen, B. Brezger, T. Pfau, and J. Mlynek, *Appl. Phys. B* **65**, 755 (1997); M. Mützel, S. Tandler, D. Haubrich, D. Meschede, K. Peithmann, M. Flaspöhler, and K. Buse, *Phys. Rev. Lett.* **88**, 083601 (2002).
- [36] G. Möllenstedt and H. Düker, *Z. Phys.* **145**, 377 (1956).
- [37] J. Denschlag, D. Cassettari, A. Chenet, S. Schneider, and J. Schmiedmayer, *Appl. Phys. B* **69**, 291 (1999).
- [38] M. V. Berry and J. P. Keating, *SIAM Rev.* **41**, 236 (1999).
- [39] For the history of the Hilbert-Pólya approach, see, for example, D. Rockmore, *Stalking the Riemann Hypothesis* (Pantheon Books, New York, 2005), or J. Derbyshire, *Prime Obsession* (Penguin Books, New York, 2004).
- [40] See, for example, the special issue on *Quantum Phase and Phase Dependent Measurements*, edited by W. P. Schleich and M. S. Barnett, *Phys. Scr. T* **48** (1993).
- [41] I. Białynicki-Birula, M. Freyberger, and W. P. Schleich, *Phys. Scr. T* **48**, 113 (1993).
- [42] J. P. Dowling, *Opt. Commun.* **86**, 119 (1991).
- [43] For another approach, see J. Twamley and G. J. Milburn, *New J. Phys.* **8**, 328 (2006). They transform the coordinate system into a hyperbolic space. Then the connection between the new position and momentum variables is given by a Mellin transform, which is central to the analytical continuation of the Riemann  $\zeta$  function.
- [44] W. Schleich, M. Pernigo, and F. L. Kien, *Phys. Rev. A* **44**, 2172 (1991).
- [45] See, for example, S. Deléglise, I. Dotsenko, C. Sayrin, J. Bernu, M. Brune, J.-M. Raimond, and S. Haroche, *Nature (London)* **455**, 510 (2008).
- [46] C. Monroe, D. M. Meekhof, B. E. King, and D. J. Wineland, *Science* **272**, 1131 (1996).
- [47] G. Rempe, H. Walther, and N. Klein, *Phys. Rev. Lett.* **58**, 353 (1987).
- [48] See, for instance, G. Freiling and V. A. Yurko, *Inverse Sturm-Liouville Problems and Their Applications* (NOVA Science Publishers, New York, 2001).
- [49] G. Borg, *Acta Math.* **78**, 1 (1946).
- [50] N. Levinson, *Mat. Fys. Medd. Dan. Vid. Selsk.* **25**(9), 1 (1949).
- [51] V. A. Marchenko, *Dokl. Akad. Nauk SSSR* **72**, 457 (1950).
- [52] B. M. Levitan, *Inverse Sturm-Liouville Problems* (VNU Science Press, Utrecht, 1987).
- [53] I. M. Gel'fand and B. M. Levitan, *Trans. Am. Math. Soc.* **1**, 253 (1951).
- [54] B. Simon, *Ann. Math.* **150**, 1029 (1999).
- [55] R. Engelke, *Am. J. Phys.* **57**, 339 (1989).
- [56] A. H. Carter, *Am. J. Phys.* **68**, 698 (2000).
- [57] N. H. Abel, *J. Reine Angew. Math.* **1826**, 153 (1826).
- [58] G. Arfken, *Mathematical Methods for Physicists*, 4th ed. (Academic Press, New York, 1995), p. 929.
- [59] I. S. Gradshteyn and I. M. Ryzhik, *Table of Integrals, Series and Products* (Academic Press, New York, 1965).
- [60] C. Quigg and J. L. Rosner, *Phys. Lett. B* **71**, 153 (1977).
- [61] T. Imbo, A. Pagnamenta, and U. Sukhatme, *Phys. Rev. D* **29**, 1669 (1984).
- [62] H. Ciftci, E. Ateser, and H. Koru, *J. Phys. A* **36**, 3821 (2003).
- [63] A. K. Roy, *J. Phys. G* **30**, 269 (2004).
- [64] F. Gesztesy and L. Pittner, *J. Phys. A* **11**, 679 (1978); **11**, 687 (1978).
- [65] H. J. W. Müller-Kirsten and S. K. Bose, *J. Math. Phys.* **20**, 2471 (1979).
- [66] I. Białynicki-Birula, M. A. Cirone, J. P. Dahl, M. Fedorov, and W. P. Schleich, *Phys. Rev. Lett.* **89**, 060404 (2002).
- [67] F. J. Asturias, *Am. J. Phys.* **53**, 893 (1985).
- [68] K. Eveker, D. Grow, B. Jost, C. E. Monfort III, K. W. Nelson, C. Stroh, and R. C. Witt, *Am. J. Phys.* **58**, 1183 (1990).